



OPEN ACCESS

EDITED BY

Ruiwen Zhang,
University of Houston, United States

REVIEWED BY

Shi Xiaopeng,
Fourth Military Medical University, China
Pan Long,
General Hospital of Western Theater
Command, China
Ding Tao,
Jilin Provincial Academy of Traditional Chinese
Medicine, China

*CORRESPONDENCE

Junguo Duan,
✉ duanjg@cdutcm.edu.cn
Maryam Mazhar,
✉ maryam@swmu.edu.cn

RECEIVED 09 February 2025

ACCEPTED 21 April 2025

PUBLISHED 21 May 2025

CITATION

Wu J, Xie W, Xie Y, Mazhar M and Duan J (2025)
Integrated proteomics analysis and network
pharmacology to elucidate the mechanism of
Zhilong Huoxue Tongyu Capsule alleviate
hypertensive retinopathy in Ang II infusion
mice model.
Front. Pharmacol. 16:1573693.
doi: 10.3389/fphar.2025.1573693

COPYRIGHT

© 2025 Wu, Xie, Xie, Mazhar and Duan. This is an
open-access article distributed under the terms
of the [Creative Commons Attribution License
\(CC BY\)](https://creativecommons.org/licenses/by/4.0/). The use, distribution or reproduction in
other forums is permitted, provided the original
author(s) and the copyright owner(s) are
credited and that the original publication in this
journal is cited, in accordance with accepted
academic practice. No use, distribution or
reproduction is permitted which does not
comply with these terms.

Integrated proteomics analysis and network pharmacology to elucidate the mechanism of Zhilong Huoxue Tongyu Capsule alleviate hypertensive retinopathy in Ang II infusion mice model

Jiao Wu¹, Wen Xie², Yucen Xie¹, Maryam Mazhar^{3*} and
Junguo Duan^{4,5*}

¹Eye School of Chengdu University of TCM, Chengdu University of Traditional Chinese Medicine, Chengdu, China, ²Department of Cardiology, Affiliated Hospital of Chengdu University of Traditional Chinese Medicine, Chengdu, China, ³National Traditional Chinese Medicine Clinical Research Base and Drug Research Center, The Affiliated Traditional Chinese Medicine Hospital of Southwest Medical University, Luzhou, China, ⁴Ineye Hospital of Chengdu University of Traditional Chinese Medicine, Chengdu, China, ⁵Key Laboratory of Sichuan Province Ophthalmopathy Prevention & Cure and Visual Function Protection with TCM Laboratory, Chengdu, China

Background: Zhilong Huoxue Tongyu Capsule (ZLHXTY) has been used in clinical treatment of vascular diseases caused by hypertension over 20 years. However, the specific mechanisms by ZLHXTY alleviate hypertensive retinopathy (HR) needs to be further explored.

Materials and methods: HR mouse model was established by infusing Ang II via subcutaneously implanted osmotic mini-pumps, followed by oral administration of ZLHXTY (0.35, 0.7, 1.4 g/kg/day) 28 days for treatment. To assess the impacts of ZLHXTY on retinal neurodegeneration and vascular injury, multiple experiments such as OCTA, ERG and HE staining were performed. Subsequently, network pharmacological and 4D-label-free proteomics to clarify the potential targets and mechanisms of ZLHXTY alleviated HR. Finally, Western blot, ELISA, IF, and other techniques were utilized to detect the expression of proteins related to inflammation, oxidative stress, and NLRP3 inflammasome activation.

Results: ZLHXTY significantly alleviated retinal dysfunction, increased retinal blood flow, and mitigated pathological changes such as retinal tissues edema in HR mice. Network pharmacology indicated that ZLHXTY might exert anti-inflammatory and anti-oxidative stress effects through targets such as TNF and NF- κ B. Proteomic analysis showed that the differential proteins between the ZL group and the Ang II group were mainly enriched in the immune-inflammatory response, and the main mechanism of which might be related to the assembly of NLRP3 inflammasome. Subsequent *in vivo* experiments corroborated that ZLHXTY remarkably attenuated inflammation and oxidative stress damage in retinal tissues. Further experiments demonstrated that ZLHXTY inhibited the NLRP3/Caspase-1/GSDMD signaling pathway and related protein expression. Finally, TEM results also verified that ZLHXTY alleviated pyroptosis in retinal cells.

Conclusion: Our results suggest that ZLHXTY by regulating the NLRP3/Caspase-1/GSDMD axis, inhibiting pyroptosis, thereby relieving retinal dysfunction and vascular injury in HR mice.

KEYWORDS

Zhilong Huoxue Tongyu Capsule, traditional Chinese medicine, hypertensive retinopathy, NLRP3 inflammasome, pyroptosis

1 Introduction

Hypertension is a prevalent and leading causes of cardiovascular diseases, which exhibits high morbidity and elevated all-cause mortality (Kario et al., 2024). Chronic elevation of blood pressure leads to arteriosclerotic changes in vascular system including ocular vasculature, leading to hypertensive retinopathy (HR) (Alswailmi, 2023). This condition disrupts both the retinal nerve fiber layer and retinal microcirculation, resulting in significant retinal damage (Dziedziak et al., 2022). It is commonly exhibited in 76.6% of the patients with primary hypertension (Li et al., 2023). It is usually asymptomatic in earlier stages, while, visual field defects and blurred vision occur in the later stages of the disease (Dziedziak et al., 2022). Untreated hypertension can lead to irreversible vision loss acutely, either due to retinal pigmentary alteration following exudative retinal detachment or secondary optic atrophy following long-term papilloedema (Do et al., 2023). Nevertheless, researches have not well elucidated the molecular mechanisms underlying HR.

The innate immune system is the primary defense against pathogens and can crucially maintain homeostasis (Cheng et al., 2024). NOD-like receptor pyrin domain-containing 3 (NLRP3) is an innate immune receptor capable of recognizing pathogen-associated molecular patterns and damage-associated molecular patterns, promoting inflammasome to be formed (Kuo et al., 2022). The NLRP3 inflammasome encompasses the sensor protein NLRP3, the adaptor protein apoptosis-associated speck-like protein (ASC), and the effector protease caspase-1 (Kodi et al., 2024). NLRP3 inflammasome activation triggers pro-inflammatory cytokines (IL-1 β and IL-18) to be secreted, thereby mediating the inflammatory response (Yang et al., 2019). According to previous studies, NLRP3 upregulation is positively correlated with inflammation in HR mice, while, NLRP3 inhibition makes pro-inflammatory cytokines less secreted (Li J. et al., 2024). Nowadays, there has been more focus given to study the interaction between NLRP3 inflammasome and pyroptosis, a type of lytic programmed cell death (Coll et al., 2022). The NLRP3 inflammasome converts pro-caspase-1 into active caspase-1, cleaving the C-terminal of GSDMD and generating several N-terminal (GSDMD-NT) active spliceosome (Vande Walle and Lamkanfi, 2024). These GSDMD-NT spliceosome migrate to the cell membrane, inducing cellular perforation.

As a result, cell death is triggered and massive inflammatory substances are released (Zheng et al., 2023). Pyroptosis is related to the pathogenesis with regard to several retinal diseases (age-related macular degeneration, diabetic retinopathy, and retinal pigment epithelial degeneration) (Al et al., 2021). According to recent studies, spontaneously hypertensive rats present elevated NLRP3 and caspase-1 (Li Y. et al., 2024). On this account, pyroptosis possibly exerts a significant effect on HR. However, the precise mechanism by which NLRP3 inflammasome induced pyroptosis contributes to HR remains unclear.

Zhilong Huoxue Tongyu Capsule (ZLHXTY) is a type of traditional Chinese medicine (TCM, Patent No. 200810147774.1) enjoying a wide application in treating hypertension-associated vascular diseases (Liu et al., 2021; Zhao X. et al., 2024). The formulation primarily encompasses Astragalus membranaceus Fisch Bunge, Sargentodoxa cuneata (Oliv.) Rehd and E. H. Wilson, Cinnamomum cassia (L.) J. Presl, Hirudo nipponica Whitman, Pheretima Aspergillum (E. Perrier). Table 1 lists the specific information. The efficacy of ZLHXTY in treating hypertensive vascular diseases is supported by numerous randomized controlled trials. Several clinical studies demonstrate that ZLHXTY can improve atherosclerosis, coronary heart disease, cerebral infarction (Liu et al., 2021), and other peripheral vascular diseases, particularly HR. A review indicates that ZLHXTY primarily exerts its effects by alleviating arterial wall sclerosis and thickening, reducing lumen narrowing, and regulating lipid and blood rheology abnormalities (Liang et al., 2021). In addition, extensive basic research demonstrates that ZLHXTY can improve endothelial cell dysfunction (Bi et al., 2024), alleviate endothelial cell pyroptosis (Liu et al., 2022), and inhibit neuronal apoptosis (Geng et al., 2023). From the perspective of TCM, HR and other vascular diseases are considered similar, both attributed to Qi deficiency and blood stasis. The effective treatment strategies involve tonifying Qi, promoting blood circulation, dispelling wind and resolving stasis. ZLHXTY is a treatment developed according to the theory of Xuanfu to invigorating qi, expelling wind, activating blood and dissolving stasis. It adheres to the principles of syndrome differentiation and treatment in TCM. Mechanistically, Inhibition of inflammation and oxidative stress are hot spots in HR treatment. Interestingly, antioxidant and anti-inflammatory properties are common to ZLHXTY ingredients (Liang et al., 2021). Thus, we speculated that ZLHXTY could alleviate HR.

2 Materials and methods

2.1 Preparation of ZLHXTY

ZLHXTY were obtained from Affiliated TCM Hospital of Southwest Medical University (Luzhou, China). All herbs components had been authenticated by Prof. Qingrong Pu, director of the TCM Preparation Room at the same institution.

Abbreviations: HR, Hypertensive retinopathy; NLRP3, NOD-like receptor pyrin domain containing 3; ZLHXTY, Zhilong Huoxue Tongyu Capsule; Ang II, Angiotensin II; SBP, Systolic blood pressure; ERG, Electroretinography; OCTA, Optical coherence tomography angiography; VAD, vessel area density; VLD, vessel length density; TUNEL, Terminal deoxynucleotidyl transferase mediated nick end labeling; TEM, Transmission electron microscopy; OPs, oscillatory potentials; RGCs, loss of retinal ganglion cells; GCL, ganglion cell layer; IPL, inner plexiform layer; OPL, outer plexiform layer; ROS, reactive oxygen species; DEPs, differentially expressed proteins; BP, biological process; CC, cellular component; MF, molecular function.

TABLE 1 The detail information of Zhilong Huoxue Tongyu capsule.

| Chinese name | Latin name | Drug name | Medicalnal part | Dose (g) | Vocher specimen number |
|--------------|---|------------------|--------------------|----------|------------------------|
| Huang Qi | <i>Astragalus membranaceus</i> Fisch. ex Bunge | Astragalus | Dried Roots | 2.3 | 90802 |
| Di long | <i>Pheretima Aspergillum</i> (E.Perrier) | Earthworm | Dried whole animal | 1.7 | 190301 |
| Shui zhi | <i>Hirudo nipponica</i> Whitman | Leech | Dried whole animal | 0.32 | 190401 |
| Da xue teng | <i>Sargentodoxa cuneate</i> (Oliv.) Rehd. Et Wils | Sargentgloryvine | Dried Twig | 1.7 | 190402 |
| Gui zhi | <i>Cinnamomum cassia</i> (L.)J.Presl | Cassia | Dried Twig | 0.86 | 190801 |

The processing and preparation of the ingredients were carried out at the pharmacy department of the Hospital (Luzhou, China). Briefly, the herbs were soaked in water (1:12) for half an hour, followed by half an hour of boiling. The process was repeated three times. After filtration, a rotary evaporator was used to concentrate the combined filtrates, which underwent vacuum freeze drying to obtain a fine powder of ZLHXTY. In previous study by our group, ZLHXTY underwent ultrahigh-performance liquid chromatography electrospray ionization orbitrap tandem mass spectrometry (UPLC-HR-MS) analysis (Bi et al., 2024).

2.2 Reagents and antibodies

Angiotensin II (Ang II, A9525) was purchased from Sigma (Darmstadt, Germany). Enalapril (H32026567) was purchased from Yangzijiang Pharmaceutical (Taizhou, China). Pentobarbital sodium salt (P3761) was purchased from Sigma-Aldrich (shanghai, China). Compound Tropicamide Eye Drops (H20123453) was purchased from Shenyang Xingqi Pharmaceutical Co., Ltd. (Shenyang, China). Haematoxylin-Eosin kit (G1120) was purchased from SOLARBIO (Beijing, China). ELISA kits (IL-6:P1326, IL-18:P1553, IL-1 β :P1301) was purchased from Beyotime Biotechnology (Shanghai, China). The kits of MDA (A003-1-2), GSH (A006-2-1), GSH-px (A005-1-2), SOD (A001-3-2) and CAT (A007-1-) were all purchased from Nanjing Jiancheng Bioengineering Institute (Nanjing, China). The One Step TUNEL Apoptosis Assay Kit (C1089), the DHE Kit (S0064S), BCA protein assay kit (BL521A), RIPA buffer (BL504A), BeyoECL Plus kit (P0018S) were purchased from Beyotime Biotechnology (Shanghai, China). Antibodies includes Iba-1 (ab5076), Goat Anti-Rabbit IgG H&L (Alexa Fluor[®] 594) (ab150080), Goat Anti-Rabbit IgG H&L (Alexa Fluor[®] 488) (ab150077) were sourced from Abcam (MA, United States). The Caspase 1 antibody (22915-1-AP), VEGFA antibody (81323-2-RR), GFAP antibody (16825-1-AP), TNF- α antibody (17590-1-AP), GSDMD antibody (20770-1-AP), NF- κ B p65 antibody (10745-1-AP), IL-1 beta antibody (26048-1-AP), GAPDH antibody (10494-1-AP), goat anti-rabbit IgG antibody (b900210) were all sourced from Proteintech (Wuhan, China). The NeuN Rabbit mAb (A19086), NLRP3 Rabbit pAb (A5652) were sourced from Abclonal (Wuhan, China).

2.3 Animals

Male C57BL/6J mice (n = 75, 6–8 weeks old) came from Chengdu Gembio (SCXK 2022-034, Chengdu, China). All animals were raised in specific pathogen-free conditions, maintained at 22°C \pm 2°C with 12-h

light/dark cycle, and with free access to water and food. This study obtained the approval of the Animal Research Committee of Southwest Medical University, Luzhou, Sichuan, China (Approval No: 20241108-006). The HR model was established by subcutaneously infusing Ang II (3,000 ng/kg/min), with saline serving as the control. Ang II infusion lasted 4 weeks with the osmotic micropumps (Alzet, model 2004, Cupertino, CA), following previous description (Wang et al., 2020). Fourteen days after the subcutaneous implantation of micropump, blood pressure was measured to assess the efficacy of the model.

2.4 Grouping and treatment

All mice were randomly divided into six groups according to ear tagging using the random number table method. Saline control group (Con), HR model group (Ang II), HR model + low dose ZLHXTY (0.35 g/kg) group (ZL-LD), HR model + medium dose ZLHXTY (0.7 g/kg/day) group (ZL-MD), HR model + high dose ZLHXTY (1.4 g/kg/day) group (ZL-HD) (Mazhar et al., 2023), HR model + Enalapril Maleate Tablets (10 mg/kg/day) group (EMY) (Geng et al., 2023). ZLHXTY was administered by oral gavage beginning 1 day after HR induction, with daily dosing (200 μ L) for 28 consecutive days at 08:00 a.m. Mice in Con and Ang II group received the same volume of saline. On 28th day, all mice were administered an overdose of pentobarbital by intraperitoneal injection for euthanization. The extracted retinal were preserved at -80°C for future analysis, while others were fixed with 10% paraformaldehyde for histological staining. Serum was collected and stored at -80°C.

2.5 Systolic blood pressure (SBP) measurement

SBP in varying groups were measured with the tail-cuff device (BP-2010A, Softron, Japan). Mice were placed in a metallic restrainer for 10 min before measurement. And SBP readings were taken once the waveform stabilized. A minimum of three measurements were recorded for each mouse. Baseline SBP was assessed 1 day before surgery, and subsequent measurements were taken on days 14, 21 and 28 following Ang II or saline infusion.

2.6 Electroretinography (ERG)

ERG tests (RetiMINER-P, IRC Medical Equipment, China) were performed on the mice at day 28th. After 24 h of dark acclimation,

all mice were anesthetized appropriately and placed on an experimental table under weak red light. The two corneas were connected to different gold wire electrodes, together with the subcutaneous insertion of the common electrode into the tail, and the connection of reference electrode to the neck. We obtained the ERG recordings of the a-wave, b-wave, and Ops wave following flash stimuli of 0.01 and 3.0 cds/m².

2.7 Optical coherence tomography angiography (OCTA)

Each animal was examined using ultra-widefield swept source OCTA (BM400K BMizar, TowardPi Medical Technology Ltd., China) after 28 days experiment. The mice were subjected to abdominal anesthesia, followed by pupil dilation using compound tropicamide eye drops. Next, the mice were gently positioned on the imaging platform. Automatic mode was selected to get a clear image, OCTA data was obtained. Furthermore, the vessel area density (VAD) and the vessel length density (VLD) were calculated automatically with the built-in software.

2.8 H&E and immunohistochemical (IHC) staining

After 72 h of immobilization in eye fixative, eyeball tissues underwent ethanol dehydration, xylene clearing, and paraffin-embedding. Subsequently, the 4 μm slices received H&E staining following standard protocols. For IHC staining, sections received the incubation of primary antibodies against Iba-1 (1:500) and Caspase 1 (1:100), and appropriate secondary antibodies. Images were captured with K-viewer software (version 1.5.3.1, KFBIO, Ningbo, China), at the optic nerve head 500 μm.

2.9 Enzyme-linked immunosorbent assay (ELISA)

ELISA kits was employed for measuring IL-6, IL-18, IL-1β serum levels as per the producer's protocol.

2.10 Antioxidant activity assays

Homogenized retinal tissues were centrifuged to isolate the supernatants. The levels of MDA, GSH, GSH-px, SOD, and CAT in retinal tissues were quantified by virtue of commercially available kits, as per the producer's protocol.

2.11 TUNEL staining

After dewaxing in xylene, paraffin sections underwent hydration through a graded alcohol series. The One Step TUNEL Apoptosis Assay Kit was adopted for retinal cell apoptosis as per the manufacturer's protocol. Fluorescence was

detected in 565 nm under fluorescence microscope (Leica DM4 B).

2.12 Immunofluorescence (IF) and DHE staining

Paraffin slices underwent antigen retrieval and 1 h of blockage in 5% BSA in succession. The slices received one night of incubation at 4°C using primary antibodies: NeuN Rabbit mAb (1:100), VEGFA (1:400), GFAP (1:100), TNF-α (1:200), NLRP3 (1:100), GSDMD (1:100), and another 2 h of incubation using secondary antibodies conjugated to Alexa594 (1:200) or Alexa488 (1:200) at room temperature. For DHE staining, the fresh frozen eyeball slices were with DHE for 30 min at RT. The last step was the 5 min of DAPI staining for nucleus. A fluorescence microscope (Leica DM4 B, Germany) was employed for capturing relevant images, and the Image J software (National Institutes of Health, United States) served for detecting the fluorescence intensity.

2.13 Western blot analysis

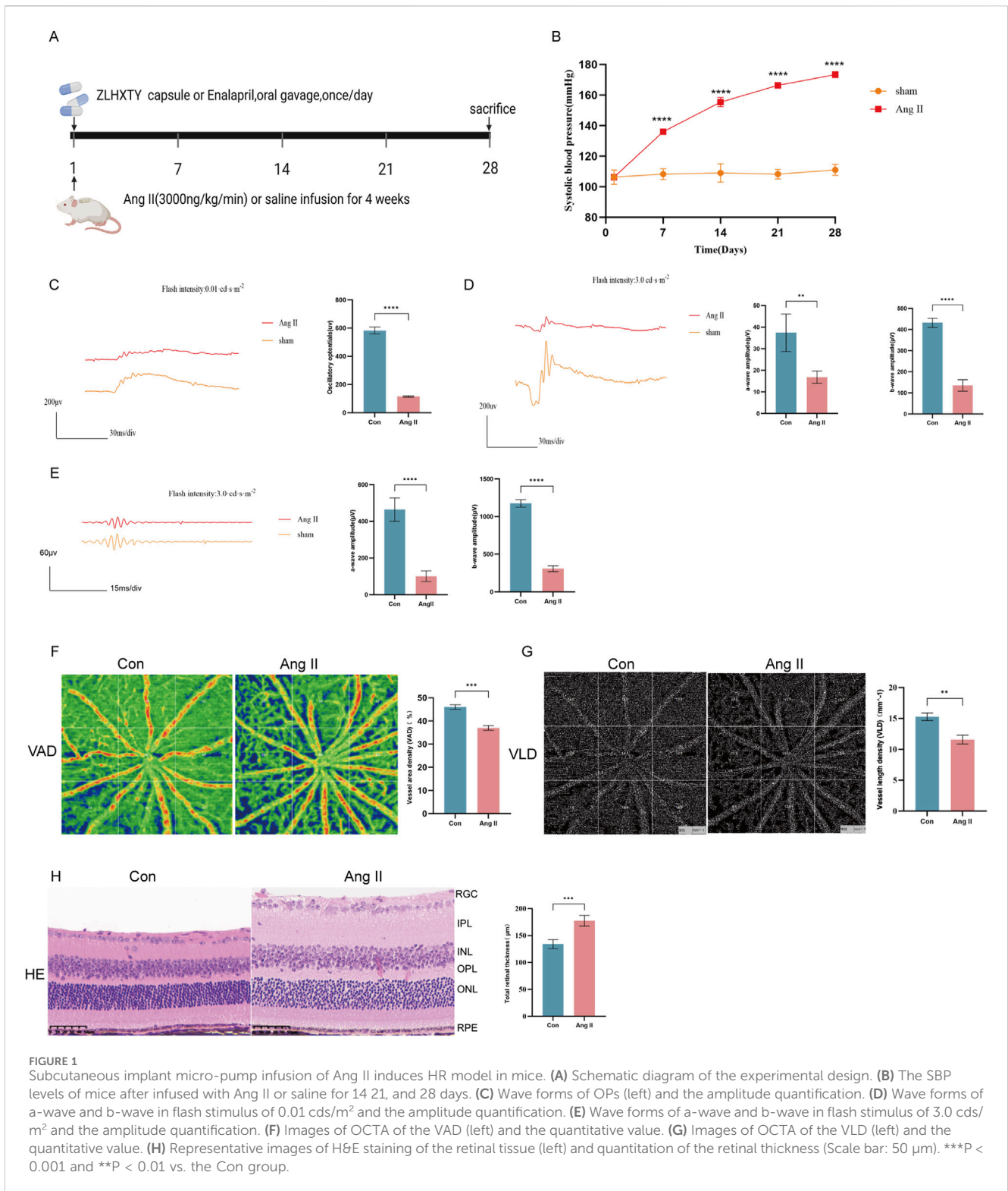
Retinal tissue samples underwent lysis treatment in RIPA buffer. BCA protein assay kit served for quantifying the protein concentration. After SDS-PAGE separation, proteins were moved to PVDF membranes. The blots received 1 h of blockage in 5% skimmed milk at RT and additionally one night of incubation using primary antibodies at 4°C: NF-κB p65 (1:1,000), TNF-α (1:1,000), IL-1β (1:1,000), and GAPDH (1:1,000). The following day, the blots underwent 1 h of incubation using horseradish peroxidase-labeled goat anti-rabbit IgG antibody (1:5,000) at room temperature. An enhanced chemiluminescence detection kit served for band visualization and the Tanon 5200 Automatic Chemiluminescence Imaging System (ChemiScope Capture, Shanghai, China) served for band analysis. Quantification was performed using ImageJ software.

2.14 Transmission electron microscopy (TEM)

After the execution of mice, the whole eyeballs underwent fixation treatment in 3% glutaraldehyde, and post-fixation in 1% osmium tetroxid. After dehydration via acetone solutions, the tissue underwent Epon 812 resin-embedding. A Leica UC7 ultramicrotome (Leica, Germany) was employed to obtain 60–90 nm ultrathin sections. Post-staining was performed for 10 min with 5% uranyl acetate, followed by 5 min of staining with Reynolds' lead citrate. Examination of the prepared sections was conducted via a TEM (JEM-1400FLASH, Japan).

2.15 4D label-free quantitative proteomic analyses

Mouse retinal tissue received 4D-label-free quantitative proteomic analysis (Zhongke New Life Biotechnology, Shanghai, China). Briefly, SDT buffer (4% SDS, 100 mM Tris-HCl) was employed for protein extraction, and trypsin (MS Grade,



Promega, United States) was employed for protein digestion as per the filter-aided sample preparation (FASP) protocol (Matthias Mann). After desalting treatment on C18 cartridges (Empore™ SPE, Sigma), the resulting peptides were reconstituted in 40 μL of 0.1% (v/v) formic acid (FA) after vacuum centrifugation. After being loaded onto an analytical C18-reversed phase column, peptides received linear gradient separation using buffer A (0.1%

formic acid in water) and buffer B (84% acetonitrile, 0.1% FA) at 300 nL/min flow rate. Mass spectrometry adopted positive ion mode, with MS data obtained by virtue of a data-dependent top 20 method, engaging in the dynamic selection of the most plentiful precursor ions for HCD fragmentation (300–1,800 m/z). We set the automatic gain control (AGC) target to 1e6, with a max injection time of 50 ms and a dynamic exclusion duration of 30 s, followed by

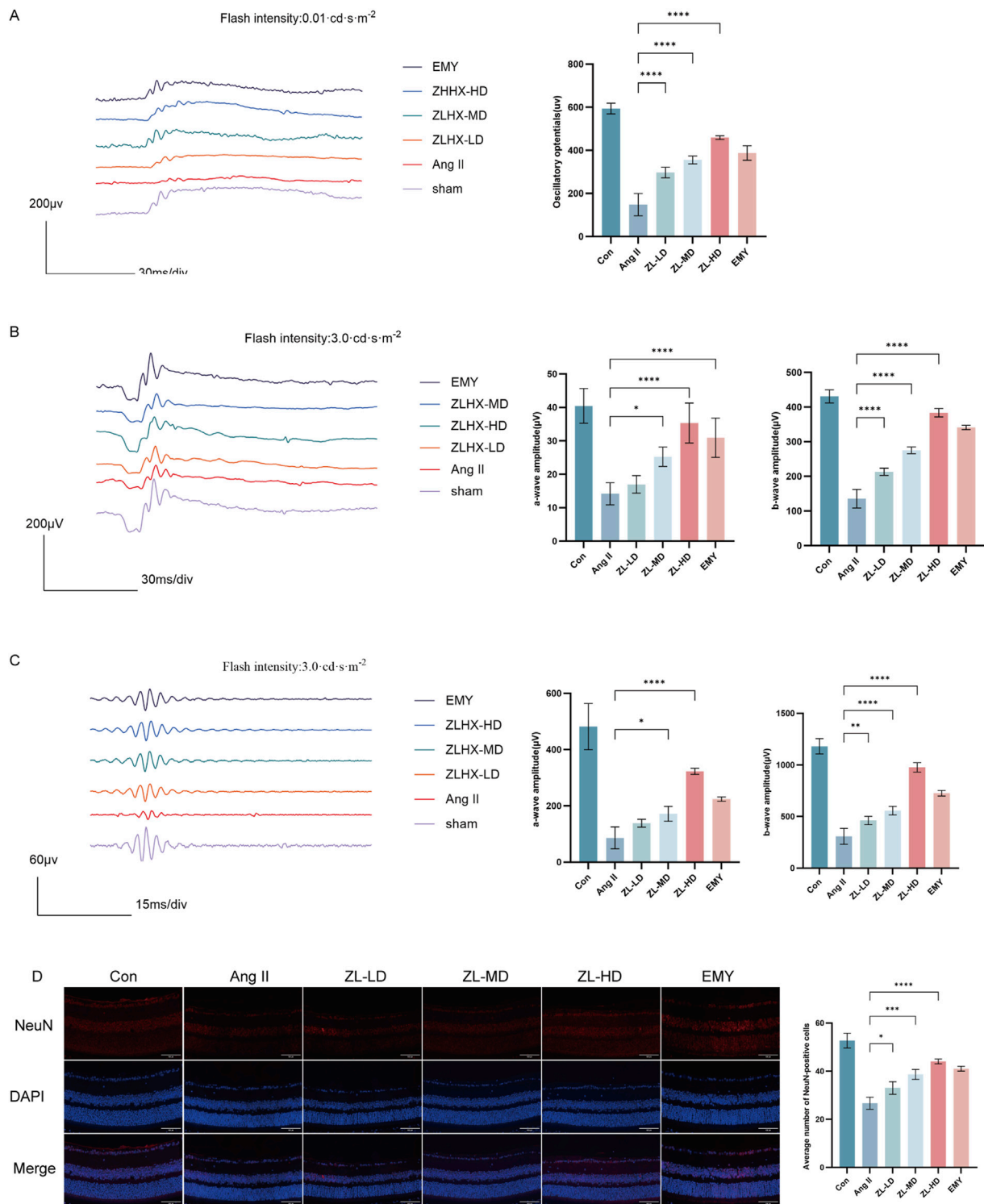
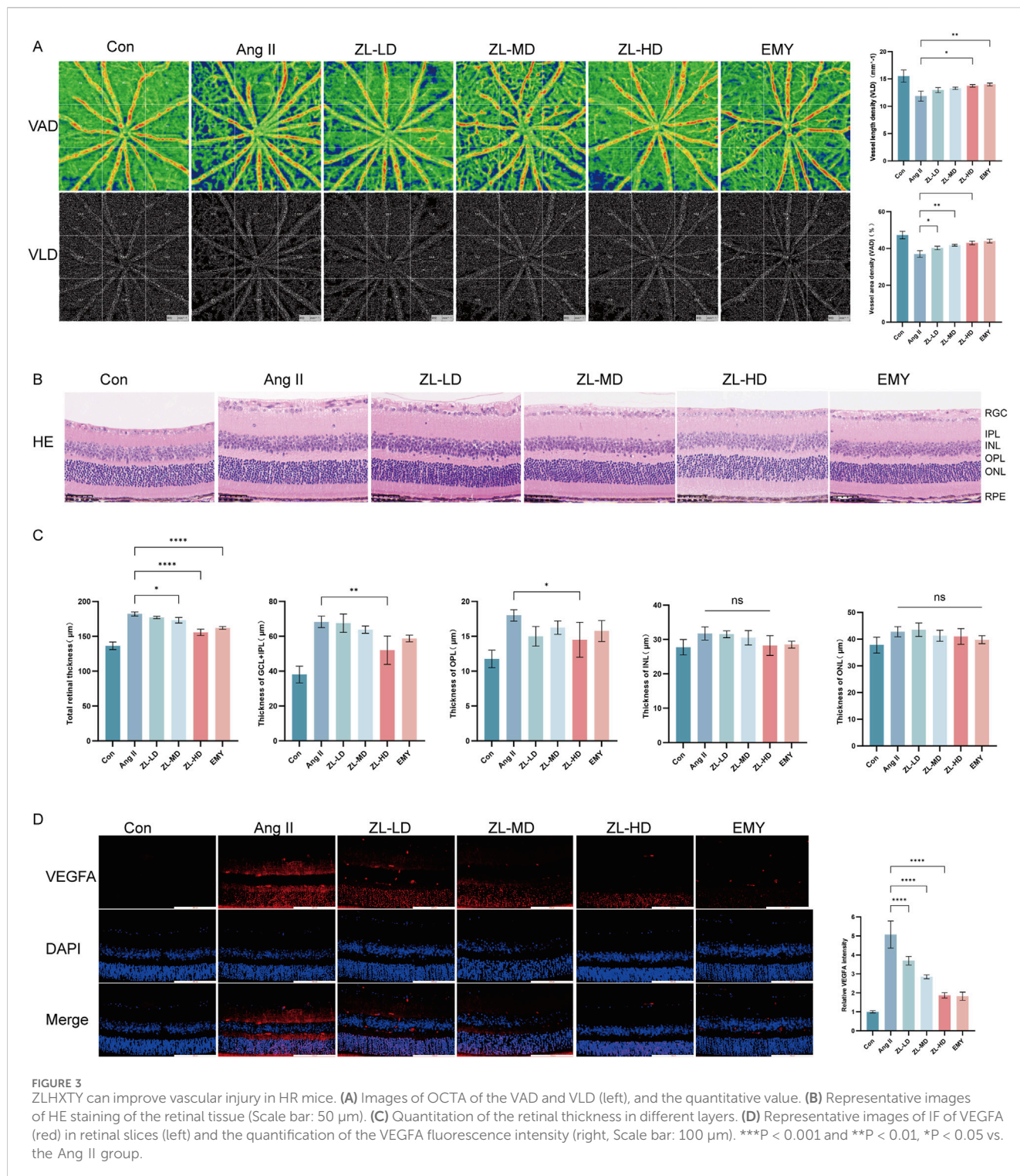


FIGURE 2 ZLHXTY alleviates retinal dysfunction in HR mice. **(A)** Wave forms of OPs (left) and the amplitude quantification. **(B)** Wave forms of a-wave and b-wave in flash stimulus of 0.01 cds/m² (left) and the amplitude quantification. **(C)** Wave forms of a-wave and b-wave in flash stimulus of 3.0 cds/m² (left) and the amplitude quantification. **(D)** Representative images of IF of NeuN (red) in retinal slices (left) and the quantification of IF intensity. ***P < 0.001 and **P < 0.01 *P < 0.05 vs. the Ang II group.

obtaining survey scans at 60,000 resolution at m/z 200, with HCD spectra acquired at 15,000 resolution at m/z 200 and an isolation width of 1.5 m/z. We set the normalized collision energy to 30 eV,

and the underfill ratio as 0.1%. MaxQuant 1.6.14 software was adopted to process and search MA raw data to identify and quantify proteins.



2.16 Bioinformatic analyses

The NCBI BLAST + client software (ncbi-blast-2.2.28+-win32.exe) together with InterProScan were adopted for the local searching of the protein sequences pertaining to the identified DPEs, aiming at confirming homologous sequences.

The procedure was followed by the assigning of GO terms, and the annotation of sequences by virtue of the Blast2GO software. Then, we queried the proteins from the KEGG database (<http://geneontology.org/>) for the acquisition of corresponding KEGG orthology identifiers, and mapped them to relevant biological pathways in KEGG.

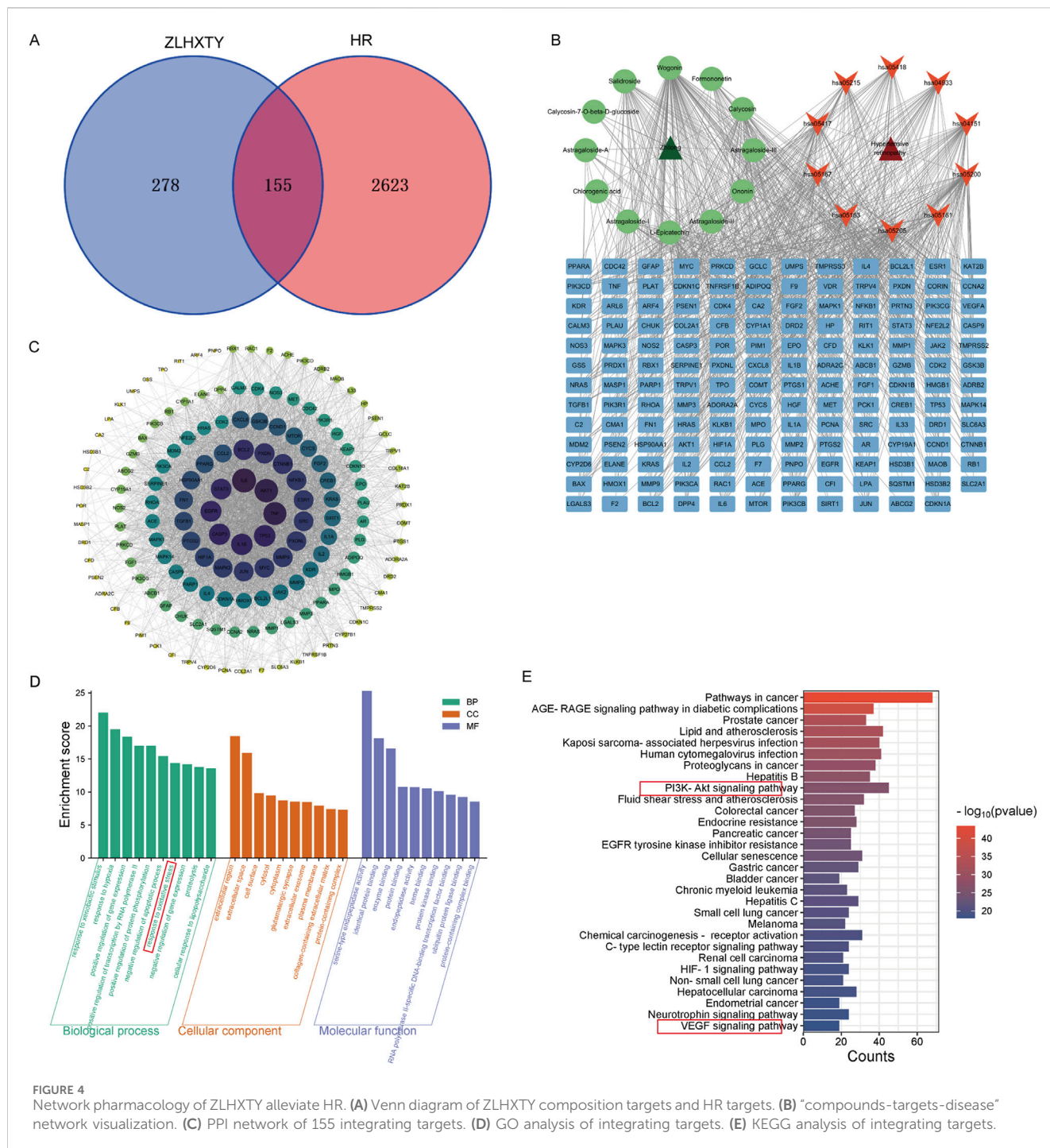


FIGURE 4 Network pharmacology of ZLHXTY alleviate HR. **(A)** Venn diagram of ZLHXTY composition targets and HR targets. **(B)** “compounds-targets-disease” network visualization. **(C)** PPI network of 155 integrating targets. **(D)** GO analysis of integrating targets. **(E)** KEGG analysis of integrating targets.

2.17 Network pharmacology

Based on previous HPLCHR-MS results, 12 compounds in ZLHXTY target prediction were performed by HERB database (<http://herb.ac.cn/>) and Swiss target prediction database (<http://www.swisstargetprediction.ch/>). The Genecards database (<https://www.genecards.org/>) was utilized to screen for targets associated with disease, “hypertensive retinopathy” as the keyword. The intersecting targets between ZLHXTY and HR were acquired by drawing the Venn diagram (Venny2.1.0 software).

The composition of ZLHXTY and the intersecting targets were introduced into Cytoscape 3.10.1 to construct the “component-target-disease” interaction network, with different node colors representing components, target genes. The intersecting targets of ZLHXTY and HR were imported into STRING (<https://string-db.org/>) to construct a protein-protein interaction (PPI) network. With the confidence level set at ≥ 0.4 , the results file in TSV format was downloaded and then imported into Cytoscape 3.10.2 software. The degree of each node was calculated using the “Tools-NetworkAnalyze” function. Core targets were selected based on three centrality metrics: betweenness centrality (BC), degree

centrality (DC), and closeness centrality (CC). The intersecting targets of ZLHXTY and HR were imported into the DAVID database (<http://david.nifcrf.gov/>) for Gene Ontology (GO) functional enrichment analysis and Kyoto encyclopedia of genes and genomes (KEGG) pathway enrichment analysis.

2.18 Statistical analysis

Data presentation followed the means \pm SEM format. Data analysis relied on GraphPad Prism 10.1.2 (GraphPad Software Inc., San Diego, United States). One-way ANOVA together with Tukey's *post hoc* test assisted in assessing the group difference. $P < 0.05$ indicates statistical significance.

3 Results

3.1 Ang II infusion induces HR mice

We used a classic subcutaneous implant micro-pump infusion of Ang II to establish a mouse model of HR (Figure 1A). As expected, 2 weeks of Ang II infusion later, the SBP in mice reached 150 mmHg (Figure 1B), meeting the standard criteria for HR modeling. Retinal neurodegeneration is an early feature of HR, and oscillatory potentials (OPs) indicate the early-stage retinal circulation disorder. On day 28th, we performed ERG tests, that revealed significant reduction in a-wave, and b-wave amplitudes in different flash stimuli (Figures 1C,D), OPs (Figure 1E) in Ang II infused HR mice. Retinal vascular injury is another early feature of HR. To evaluate the vascular changes, we performed OCTA, that revealed significantly decreased VAD (Figure 1F), large area of blue region in Ang II group and VLD (Figure 1G) in Ang II infused mice. H&E staining revealed pathological changes in retina such as edema with disordered and sparse arrangement of the retinal cells after Ang II infusion in mice (Figure 1H). These findings collectively confirmed the successful establishment of the HR model.

3.2 ZLHXTY alleviates retinal dysfunction in HR mice

On day 28th, the effects of ZLHXTY on HR visual function were assessed by analysis of ERG changes. ERG tests clearly demonstrated that the decrease in both a-wave and b-wave amplitudes in different flash stimuli markedly rescued after treatment with ZLHXTY (Figures 2A,B). Consistent with this, the reduction in Ops amplitudes was also reversed after treatment with ZLHXTY (Figure 2C). Recent research indicates that retinal function is partially linked to retinal ganglion cells (RGCs) loss (Zeng et al., 2023). The Ang II Group exhibited obviously weaker cell density of NeuN + cells in RGCs versus the Con group and the ZLHXTY group (Figure 2D). Even the ZL-HD group had a better protection effect than EMY group. Overall, the above findings suggest that ZLHXTY alleviate retinal dysfunction by protecting the loss of RGCs in HR mice.

3.3 ZLHXTY can improve vascular injury in HR mice

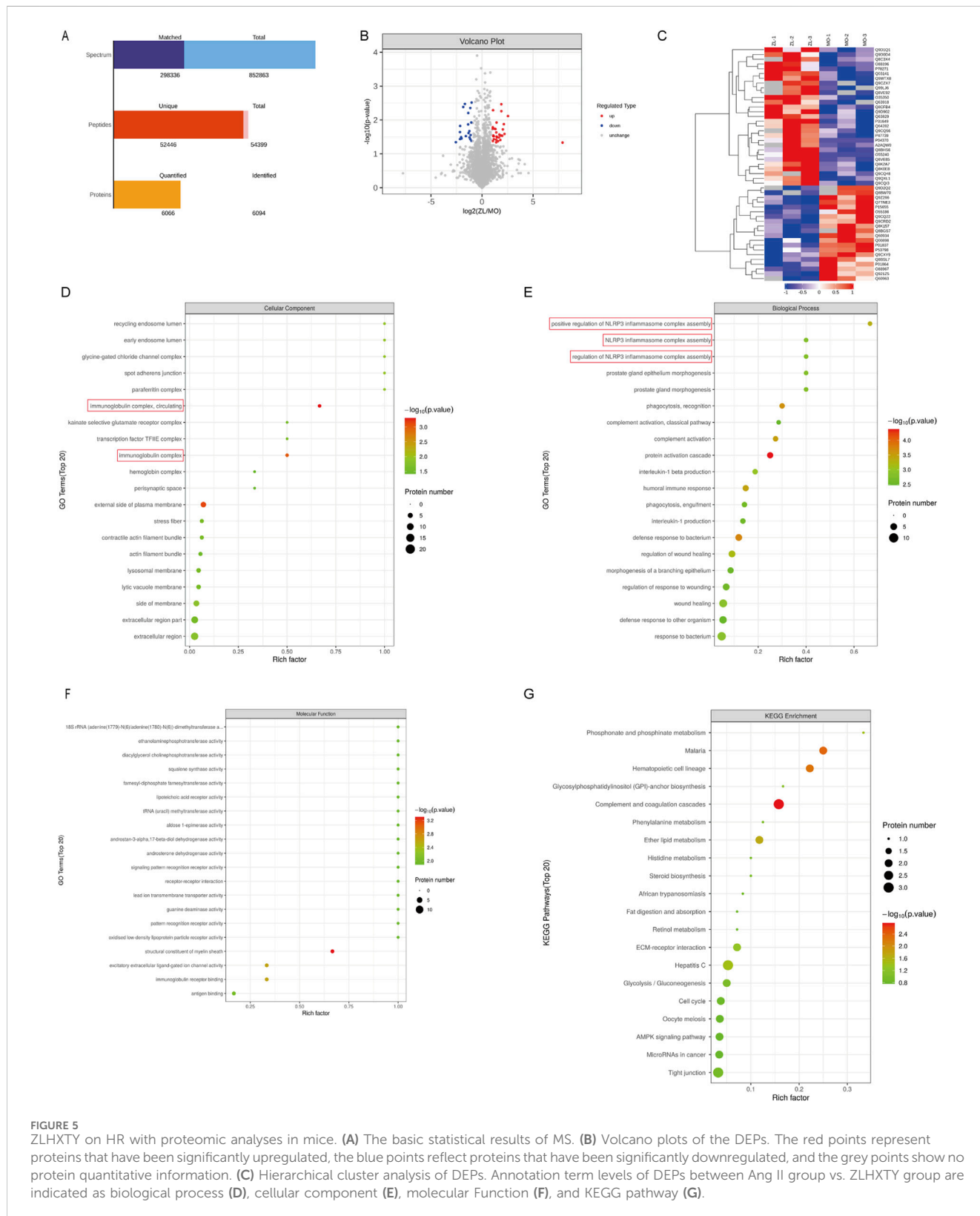
According to OCTA, VAD and VLD in ZLHXTY group were significantly increased than in Ang II group (Figure 3A). In addition, HE staining also showed that ZLHXTY treatment significantly alleviated retinal structural damage, decreased central retinal thickness, notably the thickness of the ganglion cell layer (GCL) + inner plexiform layer (IPL) and outer plexiform layer (OPL), versus the Ang II group (Figures 3B,C). The increased vascular permeability critically marks the retinopathy, while VEGFA can essentially drive the vascular permeability (Uemura et al., 2021). The IF staining for VEGFA showed increased expression in retinal samples in Ang II group, but was reduced in the ZLHXTY treated mice (Figure 3D). Taken together, these results indicate that ZLHXTY can alleviate retinal vascular injury in HR mice by inhibiting VEGFA expression.

3.4 Network pharmacology analysis

Based on the previous HPLCHR-MS results, a total of 433 targets were identified for 12 compounds of ZLHXTY. Meanwhile, 2,718 HR-related targets were obtained through the disease database. By integrating the HR-related targets and the ZLHXTY-related targets, 155 intersecting targets were successfully obtained (Figure 4A). To further explore the mechanism of ZLHXTY alleviate HR, we use Cytoscape 3.10.1 software to construct "component-target-disease" network. Degrees of freedom analysis revealed that Wogonin exhibited higher values than others among the active compounds (Figure 4B). In order to investigate the PPI among the 155 intersecting targets, a PPI analysis was carried out. Based on the betweenness BC, DC, and CC values, the top 10 core targets were identified, namely IL-6, AKT1, TNF, TP53, IL-1 β , CASP3, EGFR, STAT3, BCL2, NF- κ B1, as illustrated in Figure 4C. GO enrichment analysis revealed that intersecting targets were primarily involved in response to oxidative stress, response to hypoxia, extracellular region, serine-type endopeptidase activity (Figure 4D). Additionally, KEGG enrichment analysis emphasized the significant enrichment in pathways such as PI3K-Akt signaling pathway, VEGF signaling pathway, HIF-1 signaling pathway (Figure 4E).

3.5 Mechanisms of ZLHXTY on HR in mice with proteomic analyses

To unravel the mechanism of ZLHXTY in HR, we adopted 4D label-free quantitative proteomic analysis to confirm differentially expressed proteins (DEPs) in the retina of Con, Ang II and ZL three groups. Considering the outcomes of animal experiments, the ZL-HD group underwent the proteomic studies. According to principal component analysis, these groups present remarkably different protein expressions. Based on these qualified data, total of 6,094 proteins were identified, 6,066 of them meeting the quantitative requirements (Figure 5A). Taking a fold change >2.0 times and $p < 0.05$ as thresholds, we identified 38 upregulated and 36 downregulated proteins in Ang II group versus Con group (Table 2). A volcano plot was drawn to display these



DEPs (Figure 5B). For achieving a better visualization of the protein abundance difference, DEPs were subjected to a hierarchical clustering analysis (Figure 5C). Specifically, different proteins in cluster 3 showed a clear upregulation in Ang II group, but an obvious downregulation in

ZL group. GO and KEGG pathway analyses reveal the biological and function pathways pertaining to DEPs. Three sets of ontologies, i.e., biological process (BP), cellular component (CC), and molecular function (MF) were adopted for the individual analysis of the DEPs. In

TABLE 2 Identification differentially expressed proteins of Ang II group and ZL group.

| Gene Name | Protein ID | Protein Name |
|--------------------------------|------------|---|
| up-regulated proteins | | |
| Mbp | P04370 | Myelin basic protein |
| Rbm4b | Q8VE92 | RNA-binding protein 4B |
| Kif21b | Q9QXL1 | Kinesin-like protein KIF21B |
| Slc6a13 | P31649 | Sodium- and chloride-dependent GABA transporter 2 |
| Gpx7 | Q99LJ6 | Glutathione peroxidase 7 |
| Gbp5 | Q8CFB4 | Guanylate-binding protein 5 |
| Pip4p2 | Q9CZX7 | Type 2 phosphatidylinositol 4,5-bisphosphate 4-phosphatase |
| Mark3 | Q03141 | MAP/microtubule affinity-regulating kinase 3 |
| Guf1 | Q8C3X4 | Translation factor Guf1, mitochondrial |
| Nudcd2 | Q9CQ48 | NudC domain-containing protein 2 |
| Cavin2 | Q63918 | Caveolae-associated protein 2 |
| Use1 | Q9CQ56 | Vesicle transport protein USE1 |
| Armcx3 | Q8BHS6 | Armadillo repeat-containing X-linked protein 3 |
| Ttc3 | O88196 | E3 ubiquitin-protein ligase TTC3 |
| Aldh3a1 | P47739 | Aldehyde dehydrogenase, dimeric NADP-preferring |
| Capn1 | O35350 | Calpain-1 catalytic subunit |
| Commd3 | Q63829 | COMM domain-containing protein 3 |
| Preli3a | Q8VE85 | PRELI domain containing protein 3A |
| Mphosph6 | Q9D1Q1 | M-phase phosphoprotein 6 |
| Map3k15 | A2AQW0 | Mitogen-activated protein kinase kinase kinase 15 |
| Gtf2e2 | Q9D902 | General transcription factor IIE subunit 2 |
| Ints10 | Q8K2A7 | Integrator complex subunit 10 |
| Dimt1 | Q9D0D4 | Probable dimethyladenosine transferase |
| Pdlim4 | P70271 | PDZ and LIM domain protein 4 |
| Ifit1 | Q64282 | Interferon-induced protein with tetratricopeptide repeats 1 |
| Mad1l1 | Q9WTX8 | Mitotic spindle assembly checkpoint protein MAD1 |
| Rdh5 | O55240 | Retinol dehydrogenase 5 |
| Gmfb | Q9CQI3 | Glia maturation factor beta |
| Fgb | Q8K0E8 | Fibrinogen beta chain |
| down-regulated proteins | | |
| Usp38 | Q8BW70 | Ubiquitin carboxyl-terminal hydrolase 38 |
| Fdft1 | P53798 | Squalene synthase |
| Snapi | Q9Z266 | SNARE-associated protein Snapin |
| Lamtor1 | Q9CQ22 | Ragulator complex protein LAMTOR1 |
| Spag7 | Q7TNE3 | Sperm-associated antigen 7 |
| Arf2 | Q8BSL7 | ADP-ribosylation factor 2 |
| Cd59a | O55186 | CD59A glycoprotein |

(Continued on following page)

TABLE 2 (Continued) Identification differentially expressed proteins of Ang II group and ZL group.

| Gene Name | Protein ID | Protein Name |
|-----------|------------|--|
| Serpina1e | Q00898 | Alpha-1-antitrypsin 1-5 |
| Pigk | Q9CXY9 | GPI-anchor transamidase |
| Grik1 | Q60934 | Glutamate receptor ionotropic, kainate 1 |
| Trmt44 | Q9D2Q2 | Probable tRNA (uracil-O(2)-)-methyltransferase |
| Pla2g7 | Q60963 | Platelet-activating factor acetylhydrolase |
| Igkc | P01837 | Immunoglobulin kappa constant |
| Fgf2 | P15655 | Fibroblast growth factor 2 |
| Yme1l1 | O88967 | ATP-dependent zinc metalloprotease YME1L1 |
| Emc2 | Q9CRD2 | ER membrane protein complex subunit 2 |
| Cept1 | Q8BGS7 | Choline/ethanolaminophosphotransferase 1 |
| | P01864 | Ig gamma-2A chain C region secreted form |
| Galm | Q8K157 | Galactose mutarotase |
| Tnfaip8 | Q921Z5 | Tumor necrosis factor alpha-induced protein 8 |

Figures 5D–F, the DEGs in MF were in “immunoglobulin receptor binding”, those in CC were in “immunoglobulin complex, circulating”, “immunoglobulin complex”, and those in BP were in “protein activation cascade”, “phagocytosis, recognition”, “humoral immune response”, “positive regulation of NLRP3 inflammasome complex assembly”, “interleukin-1 beta production”, “regulation of NLRP3 inflammasome complex assembly”, “NLRP3 inflammasome complex assembly”, “phagocytosis, engulfment”, “interleukin-1 production”. Moreover, the KEGG pathway analysis demonstrates the principal involvement of the DEPs in complement and coagulation cascades, and AMPK signaling pathway (Figure 5G). Thus, in summary, the mechanism of ZLHXTY treatment of HR may be related to immune-inflammatory regulation and oxidative stress, and activation of NLRP3 inflammasome may be the main mechanism.

3.6 ZLHXTY resist oxidative stress in HR mice

Given the crucial role of oxidative stress in HR (Wan et al., 2023), and the previous network pharmacological results also suggest that oxidative stress is involved in the mechanism of ZLHXTY therapy for HR. We adopted DHE staining for the assessment of reactive oxygen species (ROS) levels in retina. The Ang II group exhibited higher ROS level versus the Con group ($p < 0.001$), whereas, the ZLHXTY significantly reduced ROS levels ($p < 0.001$) (Figure 6A,B). Furthermore, the Ang II group exhibited considerably higher serum levels of MDA versus Con group (Figure 6C). Conversely, SOD, CAT, GSH-Px and GSH levels were significantly decreased (Figures 6D–G). ZLHXTY treatment effectively reversed these effects in all five indicators. These findings suggest that ZLHXTY alleviates oxidative stress in the HR by enhancing antioxidant enzyme activity and reducing peroxide accumulation.

3.7 ZLHXTY inhibit inflammation in HR mice

Inflammation also plays a vital role in HR (Yue and Zhao, 2020). With the aim of confirming the anti-inflammatory effect of ZLHXTY, we adopted ELISA kits for examining the serum levels of IL-6, IL-18, and IL-1 β . According to Figures 7A–C, Ang II group exhibited remarkably elevated IL-1 β , IL-18 and IL-6 levels versus Con group ($p < 0.0001$). Nevertheless, after ZLHXTY treatment, their levels were reduced ($p < 0.0001$). Müller cells and microglia, as the retina’s resident immune cells, crucially coordinate the inflammatory response (Wang et al., 2022). To further elucidate the ZLHXTY intervention mechanism in HR, we performed IF. The results presented that GFAP express primarily localized to the inner limiting membrane and retinal nerve fiber layer in Con group. However, in Ang II group, GFAP expression was significantly increased and distributed throughout the retinas. In contrast, GFAP expression was reduced in the ZL-treated group (Figure 7D). According to Iba-1 IHC results, macrophages were activated in Ang II group versus Con group, while there were less macrophages in ZL-treated mice (Figure 7E,I). Network pharmacological results suggest that NF- κ B, TNF- α are core target protein of ZLHXTY for HR treatment. The results suggested that ZLHXTY suppressed TNF- α , and NF- κ B p65 expression (Figure 7F–H). These results conclude that ZLHXTY could suppresses glial cell activation and the level of inflammation in HR mice.

3.8 ZLHXTY alleviates pyroptosis through NLRP3 inflammasome activation inhibition in HR mice

According to previous studies reported NLRP3 inflammasome involvement in pyroptosis. To investigate this, we employed

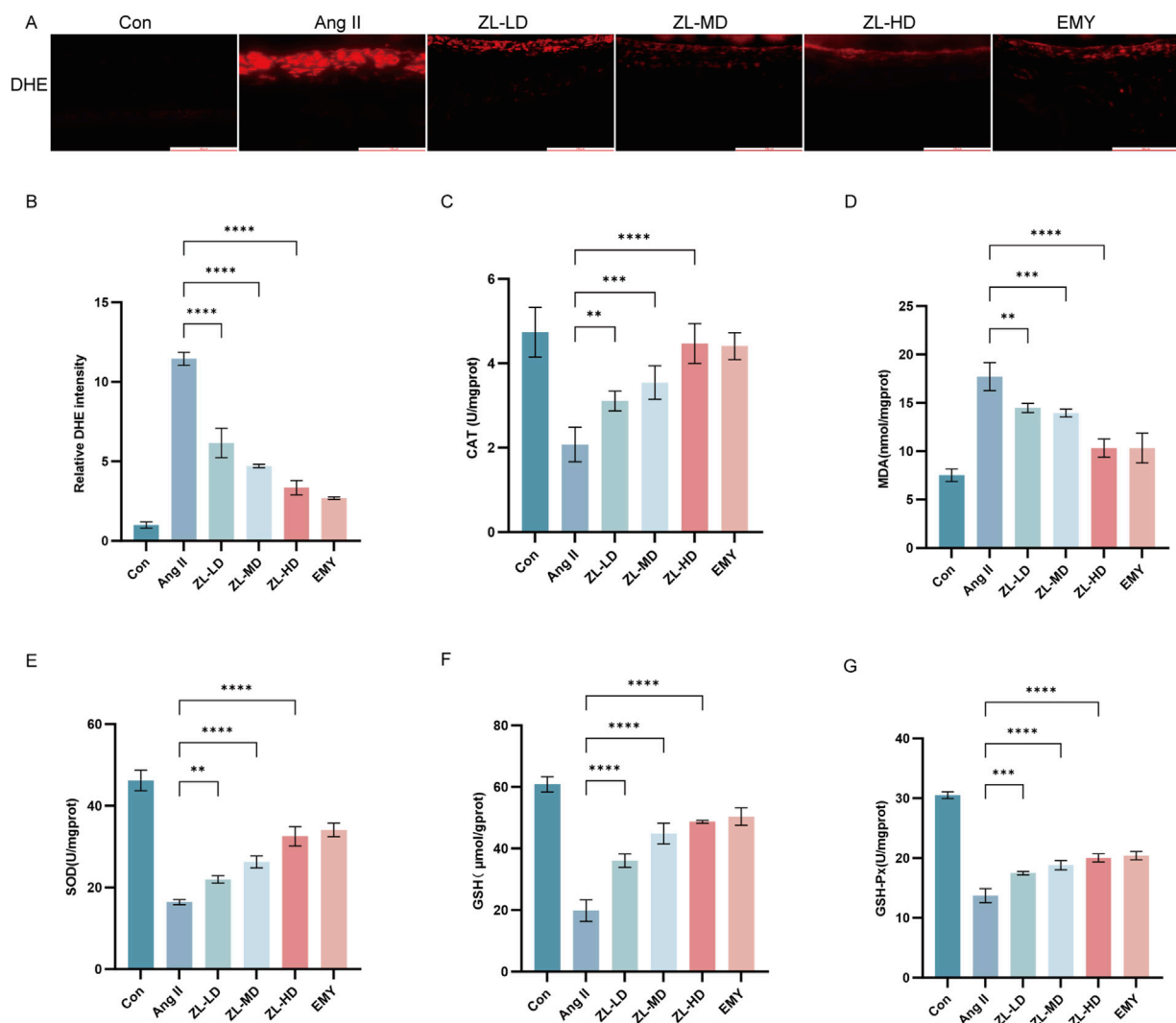


FIGURE 6 ZLHXTY resist the oxidative stress in HR mice. **(A)** Representative images of IF of DHE (red) in retina slices. **(B)** The red fluorescence intensity of DHE was quantified. **(C)** The levels of MDA in retina tissue. **(D)** The levels of SOD in retina tissue. **(E)** The levels of CAT in retina tissue. **(F)** The levels of GSH in retina tissue. **(G)** The levels of GSH-Px in retina tissue. *** $P < 0.001$ and ** $P < 0.01$ vs. the Ang II group.

TUNEL staining, ascertaining more positive cells in Ang II group versus Con group ($p < 0.0001$), while ZLHXTY treatment reduced the number of positive cells (Figure 8A). Through Western blot and IF analysis (Figures 8B–E), NLRP3, caspase-1, IL-1 β , and pyroptosis executor GSDMD presented strikingly increased protein levels versus the Con groups, whereas ZLHXTY markedly repressed the aforementioned alterations. Finally, TEM revealed that in Ang II group, many neurons showed signs of pyroptosis, with slight widening of the perinuclear space, severe loss of ribosomes in the cytoplasm, swelling and vacuolization of mitochondria, and partial expansion of the rough endoplasmic reticulum. Compared with Ang II group, there was minimal ribosomal loss in the cytoplasm, mild mitochondrial swelling, and only a few areas of discontinuity in the cell membrane in ZLHXTY group (Figures 9A–F). These findings illustrate that ZLHXTY can alleviate pyroptosis by inhibiting NLRP3 inflammasome activation.

4 Discussion

Since vascular remodeling is one of the most common signs of hypertensive organ damage, thus typical vascular injury is also among the first manifestations of HR (Wang et al., 2022). The blood-retinal barrier plays a crucial role in maintain retinal integrity and can be affected by various factors (Antonetti et al., 2021). VEGFA is a key factor contributing to blood - retinal barrier dysfunction (Dragoni and Turowski, 2018). Our study confirmed that ZLHXTY can increase retinal blood flow in HR mice. We also found that ZLHXTY can reduce the expression of VEGFA, thereby reducing vessel leakage. With the development of neurophysiological examination techniques, an increasing evidence demonstrates that retinal neurodegeneration occurs earlier than microvascular damage (Oshitari, 2021). Extensive studies have shown that in a variety of retinal diseases, the increased loss of RGCs occurs prior to microvascular injury. Moreover, the loss of RGCs is a crucial event in the process of retinal neurodegeneration

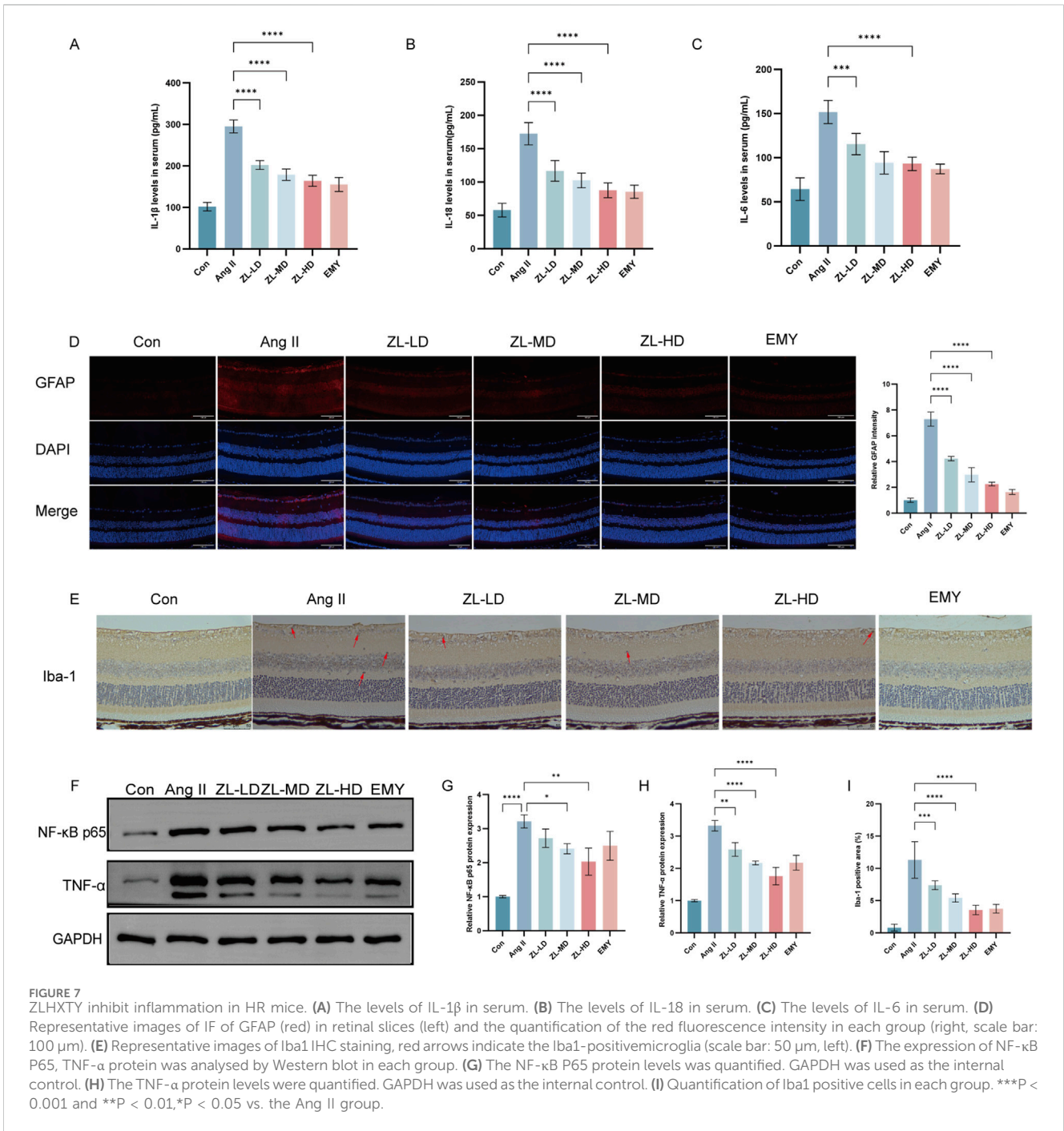


FIGURE 7 ZLHXTY inhibit inflammation in HR mice. **(A)** The levels of IL-1 β in serum. **(B)** The levels of IL-18 in serum. **(C)** The levels of IL-6 in serum. **(D)** Representative images of IF of GFAP (red) in retinal slices (left) and the quantification of the red fluorescence intensity in each group (right, scale bar: 100 μ m). **(E)** Representative images of Iba1 IHC staining, red arrows indicate the Iba1-positive microglia (scale bar: 50 μ m, left). **(F)** The expression of NF- κ B P65, TNF- α protein was analysed by Western blot in each group. **(G)** The NF- κ B P65 protein levels was quantified. GAPDH was used as the internal control. **(H)** The TNF- α protein levels were quantified. GAPDH was used as the internal control. **(I)** Quantification of Iba1 positive cells in each group. ****P < 0.001 and **P < 0.01, *P < 0.05 vs. the Ang II group.

(Wu and Mo, 2023). The hypertension milieu can cause the loss of RGCs and visual information cannot be transmitted (Farouk et al., 2021). Our results showed that ZLHXTY could alleviate the retinal neurodegeneration in HR mice by inhibiting the loss of RGCs.

Existing researches has confirmed that inflammation is a factor driving the development and progression of HR. During the pathological process of HR, due to blood exudation, lipid changes, and other factors, the retina generates a large number of inflammatory and chemotactic factors. These factors promote the migration of immune cells and trigger their excessive activation (Yue and Zhao, 2020). Activated immune cells further release

inflammatory mediators and pro-inflammatory factors, thereby exacerbating cellular damage (Zhao B. et al., 2024). Müller cell is the only cell type that spans the entire retina. Their activation is manifested by upregulated GFAP expression (Li et al., 2025). Previous studies have shown that hypertension can induce the activation of Müller cell. In the physiological state, microglial cell is in a resting state, while in the early stage of HR, it will rapidly activate and migrate to the outer nuclear layer, release inflammatory factors and triggering immune inflammatory response (Padovani-Claudio et al., 2023). In our study, Ang II infusion stimulates Müller cells and microglia to be activated, and promotes inflammatory

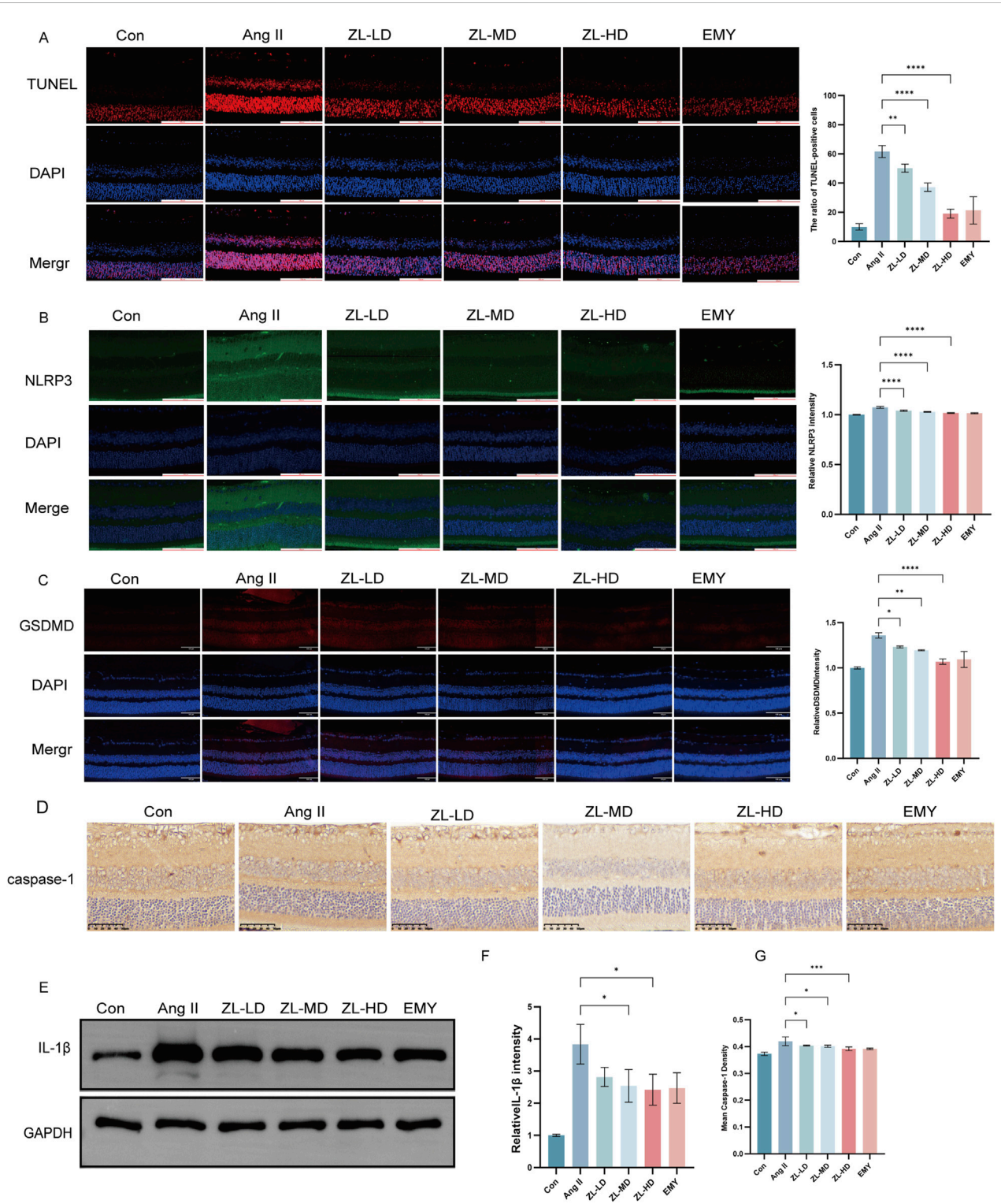


FIGURE 8 ZLHXTY alleviate apoptosis by inhibit NLRP3 inflammasome activation in HR mice. **(A)** Representative images of TUNEL (red) in retinal slices (left), and the ration of TUNEL positive cells in each group. **(B)** Representative images of IF of NLRP3 (green) in slices (left), and the quantification of the NLRP3 fluorescence intensity. **(C)** Representative images of IF of GSDMD (red) in retinal slices (left), and the quantification of the GSDMD fluorescence intensity in each group. **(D)** Representative images of IHC of caspase-1. **(E)** The expression of IL-1β protein was analysed by Western blot in each group. **(F)** The protein levels was quantified β-Action was used as the internal control. **(G)** The quantification of mean of cleaved caspase-1 density. Scale bar = 100 μm. ***P < 0.0001, and **P < 0.01, *P < 0.05 vs. the Ang II group.

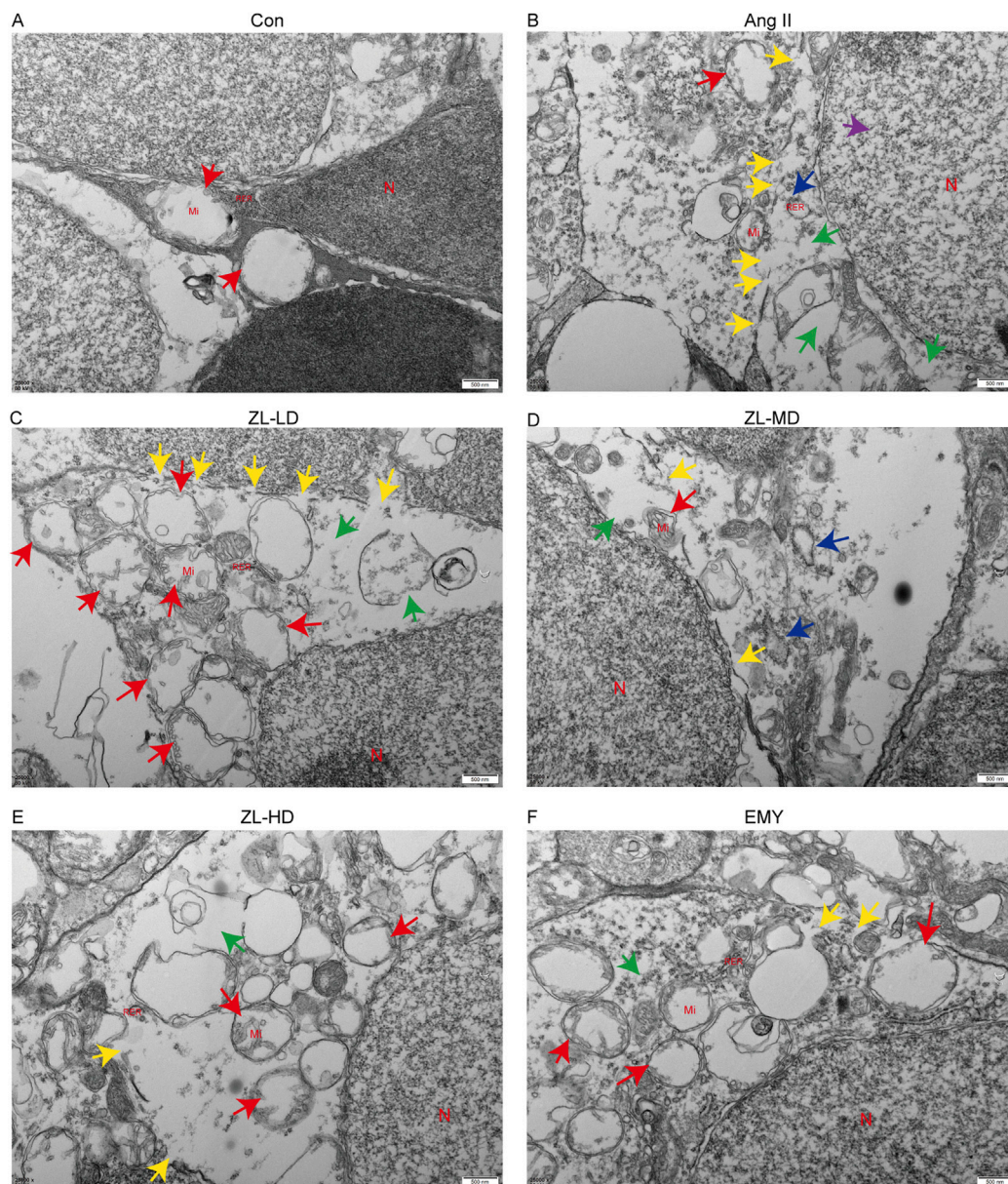


FIGURE 9

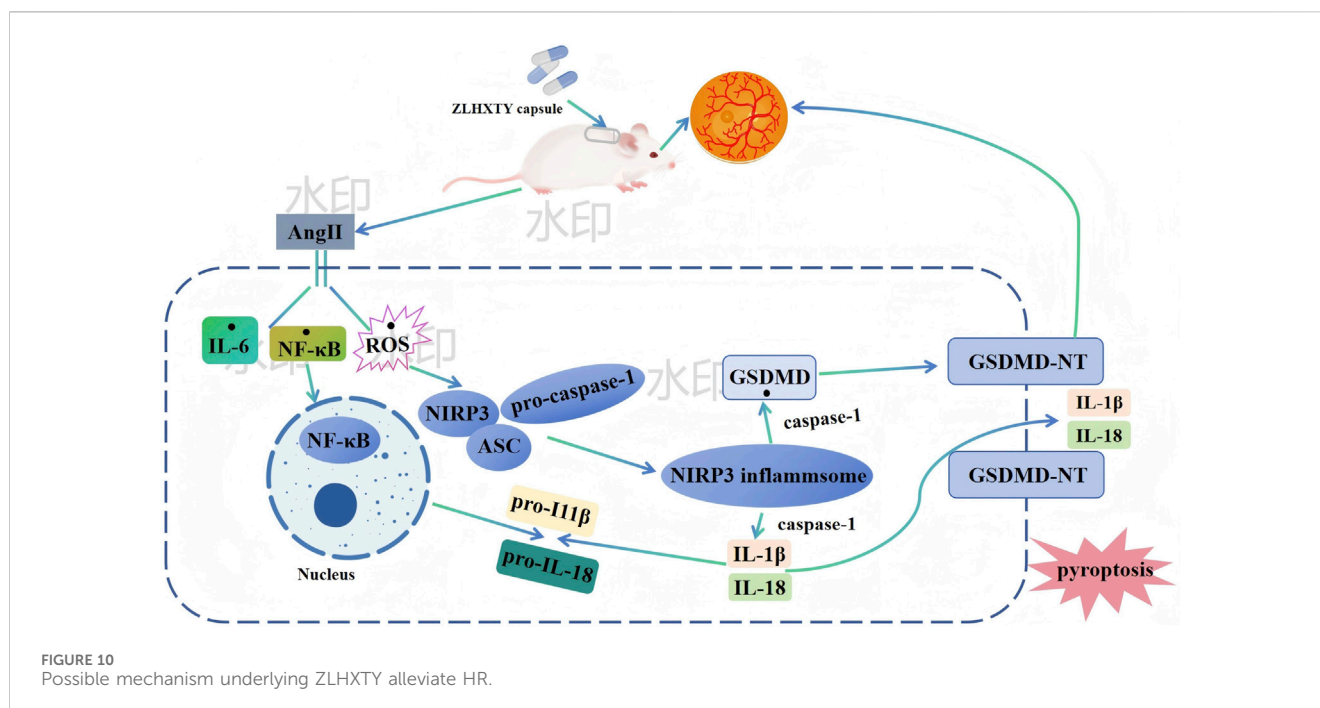
ZLHXTY alleviate apoptosis by inhibit NLRP3 inflammasome activation in HR mice. (A–F) Representative images of TEM in each group. N indicate cell nucleus, Mi indicate mitochondria, RER indicate rough endoplasmic reticulum, green arrows indicate ribosome loss, red arrows indicate mitochondrial swelling, purple arrows indicate the perinuclear space widened, blue arrows indicate trachyplasmic reticulum dilatation, yellow arrows indicate cell membrane discontinuity.

mediators (IL-18, IL-6, IL-1 β , NF- κ B, and TNF- α) to be more secreted. Treatment with ZLHXTY reversed these changes.

Oxidative stress occurs when there is an imbalance between the formation and removal of free radicals. The retina, with its high metabolic activity, is vulnerable to oxidative stress (Yang et al., 2024). According to previous studies, ROS levels increase significantly in the retina, resulting in severe oxidative stress damage (Wang et al., 2020). In our study, Ang II infusion induced ROS accumulation and made antioxidant enzymes (CAT, SOD, and GSH-Px) less activated, while increasing levels of MDA peroxidation. However, treatment with ZLHXTY

prevented these alterations. Moreover, both in network pharmacology and proteomics results suggest that the mechanism of ZLHXTY alleviate HR is closely related to inflammation and oxidative stress.

NLRP3 inflammasome plays a crucial role in triggering the inflammatory response in retinal disease. Its activation consists of two main steps: priming and (Sun et al., 2024). The priming step takes place, when Toll-like receptors detect exogenous pathogens or endogenous danger signals. This stimulus causes NF- κ B to enter the nucleus and transcription occurs, which then upregulates the expression of NLRP3 and IL-1 β (He et al., 2016). Although existing



researches have not fully elucidated the exact mechanism of NLRP3 inflammasome activation, extensive research have shown tha it is closely associated with ROS (Kuo et al., 2022). The abnormal accumulation of ROS promotes thioredoxin-interacting protein (TXNIP) to be dissociated from thioredoxin, enhancing the interaction between TXNIP and NLRP3, thus promoting NLRP3 inflammasome assembly (Fu and Wu, 2023). In recent studies, it has been found that NLRP3 expression is upregulated in HR mice, and the inhibition of NLRP3 can reduce the secretion of pro-inflammatory cytokines (Li J. et al., 2024). In our study, the expression of NLRP3 showed a marked increase after the infusion of Ang II. Conversely, upon treatment with ZLHXTY, there was a discernible decrease in NLRP3 expression. Moreover, the findings from our proteomics analysis strongly indicated that ZLHXTY predominantly exerts its regulatory effects on the NLRP3 inflammasome. Given these observations, we hypothesize that ZLHXTY mitigates the manifestations of HR by modulating the activity and function of the NLRP3 inflammasome. Recent accumulating evidence suggests that NLRP3/Caspase-1/GSDMD axis is the classic pyroptosis pathway (Gan et al., 2020). Another study has also revealed that retinal disease progresses with pyroptosis as an incipient symptom, and regulating pyroptosis can mitigate early retinal disease (Zhao et al., 2021). Our subsequent experimental results indicated that Ang II infusion effectively activates and highly upregulates the key components of the NLRP3 inflammasome complex, namely NLRP3, caspase-1, and GSDMD. However, after treatment with ZLHXTY, the expression levels of these components decreased. Finally, TEM results also showed that ZLHXTY treatment significantly alleviated pyroptosis in HR mice. Thus, the NLRP3/Caspase-1/GSDMD axis may be the molecular mechanism underlying the therapeutic effects of ZLHXTY in HR.

In conclusion, although ZLHXTY has been used in clinical treatment of hypertension-related complications for many years, existing researches have not clearly revealed the mechanism of HR. In this study, we are the first to identify ZLHXTY alleviates retinal neurodegeneration and vascular injury by inhibited pyroptosis via mediating NLRP3 inflammasome activation in HR mice. Our findings assist in understanding its potential as a target drug for HR prevention and treatment from new perspectives. However, the study has many limitations. First, we focused primarily on the effects of ZLHXTY on glial cells, neglecting other cell types. Therefore, further studies shall directly illustrate the therapeutic efficacy of ZLHXTY on other cells. Second, it has been demonstrated that ZLHXTY could blocked pyroptosis in HR mice, but the specific mechanism for such anti-apoptotic effects was not elucidated.

5 Conclusion

In conclusion, based on the findings of our study, treatment with ZLHXTY effectively alleviated retinal dysfunction and vascular injury in HR mice by inhibiting oxidative stress and inflammation in the retinal tissues. The mechanism is likely associated with the regulation of the NLRP3/Caspase-1/GSDMD axis. Specifically, ZLHXTY alleviates pyrodeath by inhibiting the activation of the NLRP3 inflammasome Figure 10. These results suggest that ZLHXTY represents a promising therapeutic approach for the management of HR.

Data availability statement

The data presented in the study are deposited in the ProteomeXchange Consortium (<https://proteomecentral.proteomexchange.org>), accession number PXD059024.

Ethics statement

The animal study was approved by the Animal Research Committee of Southwest Medical University. The study was conducted in accordance with the local legislation and institutional requirements.

Author contributions

JW: Data curation, Visualization, Writing – original draft. WX: Methodology, Project administration, Writing – review and editing. YX: Data curation, Software, Writing – original draft. MM: Conceptualization, Methodology, Supervision, Writing – review and editing. JD: Conceptualization, Funding acquisition, Supervision, Writing – review and editing. MM: Conceptualization, Methodology, Supervision, Writing – review and editing.

Funding

The author(s) declare that financial support was received for the research and/or publication of this article. This study was supported by Natural Science Foundation Project of Sichuan Provincial Department of Science and Technology: “Constructing Prediction Models for TCM Syndromes and Disease Risks Based on Network Spectral Image Information” (2021ZHYZ0017).

References

- Al, M. A., Mimi, A. A., Zaeem, M., Wu, Y., Monalisa, I., Akter, A., et al. (2021). Role of pyroptosis in diabetic retinopathy and its therapeutic implications. *Eur. J. Pharmacol.* 904, 174166. doi:10.1016/j.ejphar.2021.174166
- Alswailmi, F. K. (2023). A cross talk between the endocannabinoid system and different systems involved in the pathogenesis of hypertensive retinopathy. *Pharmaceuticals (Basel)* 16 (3), 345. doi:10.3390/ph16030345
- Antonetti, D. A., Silva, P. S., and Stitt, A. W. (2021). Current understanding of the molecular and cellular pathology of diabetic retinopathy. *Nat. Rev. Endocrinol.* 17 (4), 195–206. doi:10.1038/s41574-020-00451-4
- Bi, T., Zhou, Y., Mao, L., Liang, P., Liu, J., Yang, L., et al. (2024). Zhilong Huoxue Tongyu capsule alleviates myocardial fibrosis by improving endothelial cell dysfunction. *J. Tradit. Complement. Med.* 14 (1), 40–54. doi:10.1016/j.jtcm.2023.07.001
- Cheng, T., Yu, D., Tang, Q., Qiu, X., Li, G., Zhou, L., et al. (2024). Gender differences in the relationship between the systemic immune-inflammation index and all-cause and cardiovascular mortality among adults with hypertension: evidence from NHANES 1999–2018. *Front. Endocrinol. (Lausanne)* 15, 1436999. doi:10.3389/fendo.2024.1436999
- Coll, R. C., Schroder, K., and Pelegrin, P. (2022). NLRP3 and pyroptosis blockers for treating inflammatory diseases. *Trends Pharmacol. Sci.* 43 (8), 653–668. doi:10.1016/j.tips.2022.04.003
- Do, D. V., Han, G., Abariga, S. A., Sleilati, G., Vedula, S. S., and Hawkins, B. S. (2023). Blood pressure control for diabetic retinopathy. *Cochrane Database Syst. Rev.* 3 (3), Cd006127. doi:10.1002/14651858.CD006127.pub3
- Dragoni, S., and Turowski, P. (2018). Polarised VEGFA signalling at vascular blood–neural barriers. *Int. J. Mol. Sci.* 19 (5), 1378. doi:10.3390/ijms19051378
- Dziedzic, J., Zaleska-Żmijewska, A., Szaflik, J. P., and Cudnoch-Jędrzejewska, A. (2022). Impact of arterial hypertension on the eye: a review of the pathogenesis, diagnostic methods, and treatment of hypertensive retinopathy. *Med. Sci. Monit.* 28, e935135. doi:10.12659/MSM.935135
- Farouk, A. A., Elhadidy, R., Attia Abd Elsalam, E., Zedan, R., and Azmy, R. (2021). Role of multifocal electroretinogram in assessment of early retinal dysfunction in hypertensive patients. *Eur. J. Ophthalmol.* 31 (3), 1128–1134. doi:10.1177/1120672120934750

Acknowledgments

We are grateful to The Affiliated Traditional Chinese Medicine Hospital of Southwest Medical University for providing the components of ZLHXTY.

Conflict of interest

The authors declare that the research was conducted in the absence of any commercial or financial relationships that could be construed as a potential conflict of interest.

Generative AI statement

The authors declare that no Generative AI was used in the creation of this manuscript.

Publisher's note

All claims expressed in this article are solely those of the authors and do not necessarily represent those of their affiliated organizations, or those of the publisher, the editors and the reviewers. Any product that may be evaluated in this article, or claim that may be made by its manufacturer, is not guaranteed or endorsed by the publisher.

- Fu, J., and Wu, H. (2023). Structural mechanisms of NLRP3 inflammasome assembly and activation. *Annu. Rev. Immunol.* 41, 301–316. doi:10.1146/annurev-immunol-081022-021207
- Gan, J., Huang, M., Lan, G., Liu, L., and Xu, F. (2020). High glucose induces the loss of retinal pericytes partly via NLRP3-caspase-1-GSDMD-mediated pyroptosis. *Biomed. Res. Int.* 2020, 4510628. doi:10.1155/2020/4510628
- Geng, L., Zheng, L. Z., Kang, Y. F., Pan, C. L., Wang, T., Xie, C., et al. (2023). Zhilong Huoxue Tongyu Capsule attenuates hemorrhagic transformation through the let-7f/TLR4 signaling pathway. *J. Ethnopharmacol.* 312, 116521. doi:10.1016/j.jep.2023.116521
- He, Y., Hara, H., and Núñez, G. (2016). Mechanism and regulation of NLRP3 inflammasome activation. *Trends Biochem. Sci.* 41 (12), 1012–1021. doi:10.1016/j.tibs.2016.09.002
- Kario, K., Okura, A., Hoshida, S., and Mogi, M. (2024). The WHO Global report 2023 on hypertension warning the emerging hypertension burden in globe and its treatment strategy. *Hypertens. Res.* 47 (5), 1099–1102. doi:10.1038/s41440-024-01622-w
- Kodi, T., Sankhe, R., Gopinathan, A., Nandakumar, K., and Kishore, A. (2024). New insights on NLRP3 inflammasome: mechanisms of activation, inhibition, and epigenetic regulation. *J. Neuroimmune Pharmacol.* 19 (1), 7. doi:10.1007/s11481-024-10101-5
- Kuo, C. Y., Maran, J. J., Jamieson, E. G., Rupenthal, I. D., Murphy, R., and Mugisho, O. O. (2022). Characterization of NLRP3 inflammasome activation in the onset of diabetic retinopathy. *Int. J. Mol. Sci.* 23 (22), 14471. doi:10.3390/ijms232214471
- Li, J., Zhang, W., Zhao, L., Zhang, J., She, H., Meng, Y., et al. (2023). Positive correlation between hypertensive retinopathy and albuminuria in hypertensive adults. *BMC Ophthalmol.* 23 (1), 66. doi:10.1186/s12886-023-02807-6
- Li, J., Wang, X., Bai, J., Wei, H., Wang, W., and Wang, S. (2024). Fucoidan modulates SIRT1 and NLRP3 to alleviate hypertensive retinopathy: *in vivo* and *in vitro* insights. *J. Transl. Med.* 22 (1), 155. doi:10.1186/s12967-024-04877-6
- Li, Y., Luo, M., Chang, Q., Cao, S., Wang, Y., Chen, Z., et al. (2024). High-intensity interval training and moderate-intensity continuous training alleviate vascular dysfunction in spontaneously hypertensive rats through the inhibition of pyroptosis. *Heliyon* 10 (21), e39505. doi:10.1016/j.heliyon.2024.e39505
- Li, Z., Xiong, Q., Li, Q., and Tang, L. (2025). Parthenolide ameliorates diabetic retinopathy by suppressing microglia-induced Müller cell gliosis and inflammation via

- the NF- κ B signalling. *Int. Immunopharmacol.* 151, 114219. doi:10.1016/j.intimp.2025.114219
- Liang, P., Mao, L., Ma, Y., Ren, W., and Yang, S. (2021). A systematic review on Zhilong Huoxue Tongyu capsule in treating cardiovascular and cerebrovascular diseases: pharmacological actions, molecular mechanisms and clinical outcomes. *J. Ethnopharmacol.* 277, 114234. doi:10.1016/j.jep.2021.114234
- Liu, M., Luo, G., Liu, T., Yang, T., Wang, R., Ren, W., et al. (2022). Zhilong Huoxue Tongyu capsule alleviated the pyroptosis of vascular endothelial cells induced by ox-LDL through miR-30b-5p/NLRP3. *Evid. Based Complement. Altern. Med.* 2022, 3981350. doi:10.1155/2022/3981350
- Liu, M., Pu, Y., Gu, J., He, Q., Liu, Y., Zeng, Y., et al. (2021). Evaluation of Zhilong Huoxue Tongyu capsule in the treatment of acute cerebral infarction: a systematic review and meta-analysis of randomized controlled trials. *Phytomedicine* 86, 153566. doi:10.1016/j.phymed.2021.153566
- Mazhar, M., Yang, G., Xu, H., Liu, Y., Liang, P., Yang, L., et al. (2023). Zhilong Huoxue Tongyu capsule attenuates intracerebral hemorrhage induced redox imbalance by modulation of Nrf2 signaling pathway. *Front. Pharmacol.* 14, 1197433. doi:10.3389/fphar.2023.1197433
- Oshitari, T. (2021). The pathogenesis and therapeutic approaches of diabetic neuropathy in the retina. *Int. J. Mol. Sci.* 22 (16), 9050. doi:10.3390/ijms22169050
- Padovani-Claudio, D. A., Ramos, C. J., Capozzi, M. E., and Penn, J. S. (2023). Elucidating glial responses to products of diabetes-associated systemic dyshomeostasis. *Prog. Retin Eye Res.* 94, 101151. doi:10.1016/j.preteyeres.2022.101151
- Sun, Y., Li, F., Liu, Y., Qiao, D., Yao, X., Liu, G. S., et al. (2024). Targeting inflammasomes and pyroptosis in retinal diseases-molecular mechanisms and future perspectives. *Prog. Retin Eye Res.* 101, 101263. doi:10.1016/j.preteyeres.2024.101263
- Uemura, A., Fruttiger, M., D'amore, P. A., De Falco, S., Joussen, A. M., Sennlaub, F., et al. (2021). VEGFR1 signaling in retinal angiogenesis and microinflammation. *Prog. Retin Eye Res.* 84, 100954. doi:10.1016/j.preteyeres.2021.100954
- Vande Walle, L., and Lamkanfi, M. (2024). Drugging the NLRP3 inflammasome: from signalling mechanisms to therapeutic targets. *Nat. Rev. Drug Discov.* 23 (1), 43–66. doi:10.1038/s41573-023-00822-2
- Wan, Q., Liu, H., Xu, Y., Zhang, Q., and Tao, L. (2023). Upregulated miR-194-5p suppresses retinal microvascular endothelial cell dysfunction and mitigates the symptoms of hypertensive retinopathy in mice by targeting SOX17 and VEGF signaling. *Cell Cycle* 22 (3), 331–346. doi:10.1080/15384101.2022.2119514
- Wang, S., Bai, J., Zhang, Y. L., Lin, Q. Y., Han, X., Qu, W. K., et al. (2022). CXCL1-CXCR2 signalling mediates hypertensive retinopathy by inducing macrophage infiltration. *Redox Biol.* 56, 102438. doi:10.1016/j.redox.2022.102438
- Wang, S., Li, J., Wang, T., Bai, J., Zhang, Y. L., Lin, Q. Y., et al. (2020). Ablation of immunoproteasome β 5i subunit suppresses hypertensive retinopathy by blocking ATRAP degradation in mice. *Mol. Ther.* 28 (1), 279–292. doi:10.1016/j.ymthe.2019.09.025
- Wu, S., and Mo, X. (2023). Optic nerve regeneration in diabetic retinopathy: potentials and challenges ahead. *Int. J. Mol. Sci.* 24 (2), 1447. doi:10.3390/ijms24021447
- Yang, T. H., Kang, E. Y., Lin, P. H., Yu, B. B., Wang, J. H., Chen, V., et al. (2024). Mitochondria in retinal ganglion cells: unraveling the metabolic nexus and oxidative stress. *Int. J. Mol. Sci.* 25 (16), 8626. doi:10.3390/ijms25168626
- Yang, Y., Wang, H., Kouadir, M., Song, H., and Shi, F. (2019). Recent advances in the mechanisms of NLRP3 inflammasome activation and its inhibitors. *Cell Death Dis.* 10 (2), 128. doi:10.1038/s41419-019-1413-8
- Yue, J., and Zhao, X. (2020). GPR174 suppression attenuates retinopathy in angiotensin II (Ang II)-treated mice by reducing inflammation via PI3K/AKT signaling. *Biomed. Pharmacother.* 122, 109701. doi:10.1016/j.biopha.2019.109701
- Zeng, S., Du, L., Lu, G., and Xing, Y. (2023). CREG protects retinal ganglion cells loss and retinal function impairment against ischemia-reperfusion injury in mice via akt signaling pathway. *Mol. Neurobiol.* 60 (10), 6018–6028. doi:10.1007/s12035-023-03466-w
- Zhao, M., Li, S., and Matsubara, J. A. (2021). Targeting pyroptotic cell death pathways in retinal disease. *Front. Med. (Lausanne)* 8, 802063. doi:10.3389/fmed.2021.802063
- Zhao, B., Zhao, Y., and Sun, X. (2024). Mechanism and therapeutic targets of circulating immune cells in diabetic retinopathy. *Pharmacol. Res.* 210, 107505. doi:10.1016/j.phrs.2024.107505
- Zhao, X., Yang, F., Wu, H., Fan, Z., Wei, G., Zou, Y., et al. (2024). Zhilong Huoxue Tongyu capsule improves myocardial ischemia/reperfusion injury via the PI3K/AKT/Nrf2 axis. *PLoS One* 19 (4), e0302650. doi:10.1371/journal.pone.0302650
- Zheng, X., Wan, J., and Tan, G. (2023). The mechanisms of NLRP3 inflammasome/pyroptosis activation and their role in diabetic retinopathy. *Front. Immunol.* 14, 1151185. doi:10.3389/fimmu.2023.1151185